DFPD 90/EP/29
Padova, November 1990

C2

A study of the factors affecting the electron lifetime in ultra-pure liquid argon

A. BETTINI [4], A. BRAGGIOTTI [4]+, F. CASAGRANDE [4], P. CASOLI [4], P. CENNINI [1], S. CENTRO [4], M. CHENG [6], A. CIOCIO [2]*, S. CITTOLIN [1], D. CLINE [6], B. DAINESE [4], F. GASPARINI [5], L. MAZZONE [1], R. MUNOZ [1], G. MURATORI [4], A. PEPATO [4], G. PIANO MORTARI [3], P. PICCHI [2], F. PIETROPAOLO [4], P. ROSSI [4], C. RUBBIA [1], S. SUZUKI [4], H. WANG [2], M. ZHOU [6].

[1] *CERN, CH-1211, Geneva 23, Switzerland*
[2] *Laboratori Nazionali di Frascati dell'INFN, via Enrico Fermi 40, Frascati, Rome, Italy*
[3] *Dipartimento di Fisica e INFN, Università de l'Aquila, via Vetoio, Coppito (AQ), Italy*
[4] *Dipartimento di Fisica e Sezione dell'INFN, Università di Padova, via F. Marzolo 8, Padova, Italy*
[5] *Dipartimento di Fisica e INFN, Università di Udine, via Larga 36, Udine, Italy*
[6] *Department of Physics, UCLA, Los Angeles, CA 90024, USA*

+ *Present address : CNR, Corso Stati Uniti, Padova, Italy*
* *Present address : Physics Division, LBL, 1 Cyclotron Rd, Berkeley, CA 94720, U.S.A.*

(submitted to Nucl. Instr. Methods A)

UNIVERSITÀ DEGLI STUDI DI PADOVA
DIPARTIMENTO DI FISICA
"GALILEO GALILEI"

ISTITUTO NAZIONALE DI FISICA NUCLEARE
SEZIONE DI PADOVA

Via Marzolo, 8 - 35131 PADOVA (ITALIA)

DFPD 90/EP/29
Padova, November 1990

A study of the factors affecting the electron lifetime in ultra-pure liquid argon

A. BETTINI [4], A. BRAGGIOTTI [4]+, F. CASAGRANDE [4], P. CASOLI [4], P. CENNINI [1], S. CENTRO [4], M. CHENG [6], A. CIOCIO [2]*, S. CITTOLIN [1], D. CLINE [6], B. DAINESE [4], F. GASPARINI [5], L. MAZZONE [1], R. MUNOZ [1], G. MURATORI [4], A. PEPATO [4], G. PIANO MORTARI [3], P. PICCHI [2], F. PIETROPAOLO [4], P. ROSSI [4], C. RUBBIA [1], S. SUZUKI [4], H. WANG [2], M. ZHOU [6].

1) CERN, CH-1211, Geneva 23, Switzerland
2) Laboratori Nazionali di Frascati dell'INFN, via Enrico Fermi 40, Frascati, Rome, Italy
3) Dipartimento di Fisica e INFN, Università de l'Aquila, via Vetoio, Coppito (AQ), Italy
4) Dipartimento di Fisica e Sezione dell'INFN, Università di Padova, via F. Marzolo 8, Padova, Italy
5) Dipartimento di Fisica e INFN, Università di Udine, via Larga 36, Udine, Italy
6) Department of Physics, UCLA, Los Angeles, CA 90024, USA

+ Present address : CNR, Corso Stati Uniti, Padova, Italy
** Present address : Physics Division, LBL, 1 Cyclotron Rd, Berkeley, CA 94720, U.S.A.*

(submitted to Nucl. Instr. Methods A)

ABSTRACT

As part of the development program for the ICARUS experiment, which consists of a very large time projection chamber (TPC) filled with ultra-pure liquid Ar (LAr), we have carried out tests with different purifier systems, in order to evaluate the performance of the various parts and to improve the purification techniques developed so far.

Electron lifetime τ in LAr has been determined with an improved method based on the measurement of the attenuation of a current due to an electron cloud, photo-produced by a laser pulse impinging on a metallic cathode and moving in a small drift chamber filled with the purified LAr.

Results of the above-mentioned tests are reported. During these tests, we observed repeatedly and reproducibly an *increase* of τ that took place over a period of 10 to 20 hours after liquefaction. Several tests performed in an attempt to elucidate this effect, suggest that the increase in τ is due to adsorption of electron-attaching impurities on the walls of the stainless steel container, a process governed by thermal diffusion.

The electron lifetime monitoring system reported here was used to measure the electric field dependence of τ in purified LAr doped with O_2 and CO_2, for fields 100 V/cm < E < 800 V/cm. The results for O_2 are consistent with published data.

1. Introduction

As part of the ongoing ICARUS experiment [1,2], we have prepared an Ar purification system to fill with LAr a TPC with a volume of 2000 litres. In order to successfully accomplish this task, two of the main difficulties that must be overcome, are: (i) the purification of relatively large quantities of LAr needed to fill the chamber, with a purification system which should be modular and as simple as possible; (ii) the implementation of a fast and accurate technique to monitor the electron lifetime in the liquid, capable of operating in a noisy environment (e. g. during the liquefaction process).

For these reasons, we have undertaken a systematic study of different purification systems, in order to evaluate them and to find an optimum system capable of delivering the required quantity of high purity Ar with a minimum number of components. At the same time, we have improved a technique already developed [3] to measure the electron lifetime in LAr. This technique — which relies in the photoproduction of electrons by means of an ultraviolet (UV) laser pulse — exhibits three distinct advantages when compared with techniques used previously, based on the analysis of the output of a charge sensitive amplifier in response to the current resulting from ionization produced by the passage of minimum ionizing particles through the LAr chamber [1]. Due to the large signal to noise ratio, (a) it can be used in a very noisy environment, (b) τ can be measured rapidly, since a *single* laser pulse suffices to perform the measurement and (c) it allows measurements of τ from a few microseconds to a few milliseconds.

The purpose of the present communication is to report on the results we have obtained, concerning the two main problems (i) and (ii) mentioned above. Its content is organized as follows. In Section 2 we present a brief review of the device used to measure τ, and a short description of various improvements and modifications. Section 3 contains a discussion of how τ is extracted from the raw data, as well as a discussion of the accuracy of the measurement. In Section 4 we report on several tests performed with different Ar purification systems. During these tests, we observed repeatedly and reproducibly an increase of τ that took place over a period of 10 to 20 hours after liquefaction. In Section 5 we report on a series of tests performed in an attempt to elucidate this peculiar effect. In Section 6 we report measurements of the electric field dependence of the electron lifetime τ in purified LAr doped with O_2 and CO_2, for fields 100 V/cm < E < 800 V/cm. In Section 7 we summarize the results.

2. Experimental method

In a double gridded drift chamber an electron cloud is photoproduced by a very short UV laser pulse impinging on the cathode; these electrons drift towards the anode. Up to 10^7 electrons may be produced by a single laser pulse. The number of electrons extracted from the cathode will exceed the number of electrons arriving at the anode, after drifting across the distance separating cathode from anode. The amount by which the former exceeds the latter constitutes a measure of the proportion of electrons lost via attachment to electronegative impurities during transit from cathode to anode. Measuring the ratio between these two charges allows a determination of the electron lifetime in the liquid.

2.1 The cell and the monitoring system

The cell and the vessel are shown in Fig. 1. A schematic view of the monitoring system, including the cell and the electronic signal processing, is shown in Fig. 2.

The cell is a double gridded drift chamber with the cathode at the bottom and the anode at the top, with a total volume of 250 cc. The grid was constructed from a mesh of 100 μm diameter copper wires separated by 2 mm.

If the ratio r of the electric fields after and before the grids is higher than 1.4, then complete transparency of the grids with respect to the electrons is assured [1]. A more precise calculation performed taking into account the two dimensional structure of the mesh leads to a value r = 1.9. Thus a different value of the electric field is then needed for each of the three drift gaps. To satisfy this requirement of grid transparency, we selected a ratio r = 2.5.

A chain of metal oxide resistors on ceramic supports (72 MΩ ± 1 % at LAr temperature)[1] degrades the electric potential, and 4 high voltage cryogenic feed-throughs[2] make electrically accessible the cathode, the anode and the two grids. The high voltage is fed via 4 coaxial cables 50 cm long. To maximize the electric field in the drift region without exceeding the breakdown voltage on the feed-throughs (2 kV), a positive

---

[1] Neohm, Torino, Italy.

[2] Type Frialit, trademark of Friedrichs-Feld GmbH, Mannheim, Germany.

voltage is applied on the anode and the grid facing it, and a negative voltage is applied on the cathode and its respective grid.

The source of electrons is a photo-cathode made of a thin layer of gold (1 μm thick, 10 mm diameter) evaporated on a copper disk (1 mm thick, 18 mm diameter). Gold was chosen not only for its low work function ($W_{Au} \approx 4.9$ eV) but also because it does not oxidize easily and therefore its photoelectric characteristics do not degrade with time.

A computer simulation shows that the trajectories of the electrons extracted from the photocathode, are not influenced by the non uniformity of the electric field due to the effect of the edges (Fig. 3).

The light needed to produce the electrons is produced by a Nd-Yag laser[3]; it is brought onto the photocathode through a quartz optical fibre (≈ 100 cm long, 1.2 mm diameter) that can operate at wavelengths down to 180 nm[4] The fibre enters the chamber via a cryogenic indium sealed feed-through developed by our group and shown in Fig. 1; it ends at 5 mm from the axis of the chamber, touches the photo-cathode at an angle of 11° in order to maximize the area hit by the light.

The laser beam is focused on the optical fibre by a quartz lens with a focal distance of 10 cm. The ratio between the light intensity at the output and at the input of the fibre was measured with a joulemeter[5] , operating via the pyroelectric effect, to be about 3 %.

The electrons generated by the laser pulse drift from the cathode towards the first grid, inducing a current in the cathode. After the electron cloud crosses the first grid, the current induced in the cathode becomes approximately zero because the grid screens the cathode. Typical waveforms are shown in Fig. 4.

We find that although only 3 percent of the light emitted by the laser reaches the photocathode, the number of photoelectrons injected into the liquid is in the range $10^6 \div 10^7$; a number of electrons $\geq 10^6$ can be obtained for a wide combination of electric field and laser intensities. This is because the photon energy (E_γ) is in fact very close to the photoelectric threshold (E_{th})

$$E_\gamma = 4.66 \text{ eV}$$
$$E_{th} = W_{Au} + V_0 = (4.9 - 0.2) \text{ eV} = 4.7 \text{ eV}$$

[3] Model SL400, Spectron Laser System, U.K.
[4] Superguide G-UV, FIBERGUIDE Inc., U.S.A.
[5] Pyroelectyric Joulemeter Model J3,.Molectron Detector Inc., U.S.A.

where $V_0 = -0.2$ eV is the energy of the conduction band of the electrons in LAr [4].

All the components of the monitoring system that will be in contact with the ultra-pure Argon are cleaned following the CERN standard procedure [1,5], but avoiding halogenated solvents.

The vessel containing the drift cell is connected to a turbo-molecular pumping system through a cold trap, in order to reach a residual pressure $< 10^{-7}$ mbar, and to the ICARUS test purifier [1]. The vessel is immersed into a dewar containing the LAr bath needed to condense the gas coming from the purifier. Before each liquefaction the system is baked out under vacuum for at least 24÷48 hours at 120°C. Such relatively low baking temperature is used to avoid damage to the resistors and the fibre feed-through. After bake-out, a typical leak rate is less than 10^{-9} mbar litre sec^{-1} and the degassing rate less than 10^{-12} mbar litre sec^{-1} cm^{-2} at room temperature, compatible with the published data for stainless steel [6].

A typical filling can be completed in about 20 min. To evacuate the chamber, the Ar is evaporated through a silicon oil[6] bubbler in order to prevent contamination of the monitor due to back diffusion of air.

3. Determination of the electron lifetime τ

Let t = 0 designate the firing of a laser pulse. The charge photoinjected from the cathode travels the distance separating the cathode from the first grid in a time T_C. Since the width of the laser pulse (20 nsec) is two orders of magnitude smaller than the shortest drift time between cathode and first grid ($T_C > 7$ μsec), the distortion of the signal due to the time during which electrons are ejected from the cathode is negligible. Let Q_C be the integrated charge flowing into the cathode during the interval $0 < t < T_C$. After $t = T_C$, the electron cloud drifts across the gap separating the two grids, in a time T_D. Due to the shielding of the grids — and provided that the biasing field is such as to guarantee transparency of the grids (e. g. that no electrons are lost while traversing the grids) — no current flows into/from the cathode/anode during the period $T_C < t < T_C + T_D$. Finally, the electron cloud goes past the second grid and travels the distance separating this second grid from the anode in a time T_A. Let Q_A be the integrated charge flowing out of the anode during the interval $T_C + T_D < t < T_C + T_D + T_A$. The ratio $R = Q_A/Q_C$ is a function *only* of the drift times T_C, T_D, T_A and of the electron lifetime τ:

[6] Diffusion pump oil type 705, Dow-Corning, U.S.A.

$$R = \frac{Q_A}{Q_C} = \left[\frac{T_C \sinh(T_A/2\tau)}{T_A \sinh(T_C/2\tau)}\right] \exp\left\{-\frac{T_D + \frac{T_A+T_C}{2}}{\tau}\right\} \qquad (1)$$

If $T_C << \tau$ and $T_A << \tau$, then the right hand side of eq. (1) can be well approximated by the exponential term, since in this case the quantity in square brackets is essentially unity.

A wide set of electric fields can be used to operate the monitor, from a few V/cm to a few hundred V/cm; the corresponding drift time ranges from 30 to 300 μs. As an example, fields, voltages, and transit times are reported for two typical configurations: 400 V/cm in Table 1 and 50 V/cm in Table 2.

Equation 1 shows that τ does not depend on the absolute value of Q_A and Q_C but only on their ratio. To take advantage of this fact, only one charge sensitive amplifier was used to read Q_A and Q_C, thus avoiding errors which would arise from absolute calibration if two electronic channels were used instead. The amplifier employed to read Q_A and Q_C is a-c coupled to the anode and the cathode by two 4 KV - 4.7 nF capacitors. In order to avoid electronic distortions to the overall signal, the amplifier has a rise time of 400 ns, fast with respect to T_C and T_A, and a feedback time constant of 4 milliseconds, long compared to $(T_C + T_D + T_A)$. The resulting equivalent noise charge (ENC) is about $5 \cdot 10^3$ electrons or ≈ 0.1 % of a typical signal amplitude.

After the preamplifier, the signal is fed into a variable gain differential amplifier and then the low frequency noise is eliminated using a sample and hold circuit (Fig. 2). The resulting signal is sent to a wave form analyzer (WFA)[7], mounted in a CAMAC module. The WFA can store up to 1024 successive samples with an accuracy of 8 bits and the sampling time can vary from 50 ns to 5 μs. The linearity of the WFA is thus the only parameter that has to be checked during the measurement.

The data acquisition is controlled using a MacIntosh micro-computer[8] via a standard CAMAC Mac-CC controller and the data of each event are recorded for off-line analysis. The event rate can vary from one event every few seconds to one event every few minutes, depending on the tests to be performed.

3.1 Resolution

[7] 20 MHz WFA – CAMAC Model 2256, LeCroy, U.S.A.

[8] MacIntosh is a trademark of Apple Computer Inc., U.S.A.

Two typical output signals, recorded with the electric field configurations of tables 1 and 2 and different LAr purity levels, are shown in Fig. 4.

In the off-line analysis, each event is fitted with a 3-parameter function that has the trapezoidal shape[9] shown in Fig. 4. The fitting parameters are then Q_C, Q_A, and the time interval $T_w = T_D + (T_C + T_A) / 2$, which corresponds to the full width at half maximum of the overall signal.

Assuming that ΔR and ΔT_w are the only relevant sources of error, the resolution $\Delta\tau/\tau$ is given by

$$\frac{\Delta\tau}{\tau} = \sqrt{\left(\frac{1}{\ln(R)}\frac{\Delta R}{R}\right)^2 + \left(\frac{\Delta T_w}{T_w}\right)^2} \qquad (2)$$

In order to determine the range of ratios R over which the electron lifetime τ is measurable with an accuracy of 10% or less, in Fig. 5 we have plotted eq. (2), assuming a $\Delta T_w/T_w \sim 5\%$, typical systematic error due to the least count on the ADC in a measurement performed with a single laser shot (it is this systematic error that determines the minimum in the curve). From Fig. 5 it can be seen that the acceptable range of R (that permits a measurement of τ with an accuracy of 10% or less) turns out to be $0.08 < R < 0.76$.

This information can be used to determine the range of electron lifetimes over which the measurement of τ can be carried out with the required accuracy. For this purpose we have plotted in Fig. 6 the ratio R given by eq. (1), ignoring the term in square brackets; a plot for a minimum field (50 V/cm) and maximum field (400 V/cm) is included. From these plots it can be seen that electron lifetimes can be determined with the required accuracy for $15\ \mu s < \tau < 900\ \mu s$; this range can be extended by reducing the systematic error on the ADC's least count, this can be accomplished by averaging the signal over several laser pulses.

To cross-check the performance of the electron lifetime monitor described above, a measurement of τ was performed liquefying purified Ar in both the monitoring chamber and into the 24 cm TPC reported in Ref. 2. In the latter the electron lifetime was determined by analyzing the output of a charge sensitive amplifier in response to the current resulting from ionization produced by muon tracks parallel to the anode, generated

[9] This shape corresponds to approximating the charge ratio R by the exponential term in the right-hand side of eq. (1). When $\tau > 15$ μs, for the cell reported here, the error involved in ignoring the term in square brackets is less than 0.1%.

at different distances from it. The results of both measurements, $\tau \sim 4$ ms, agreed within experimental error.

4. Performance of different purification systems

Recall that the electron lifetimes (several milliseconds) reported earlier [1] were obtained using Ar 60 as gas source (concentration of $O_2 <$ 0.1 ppm according to the supplier), and a purification system designed for small flow (of the order of a few thousand litres of Ar gas per hour at STP). This system was comprised of a OXISORB cartridge[10] (containing Cr imbedded in a molecular sieve bed as active element); a storage reservoir for the purified liquid; and a home-made molecular sieve filter containing silica gel, and Linde 4A and 13X molecular sieves, mixed in proportion of 1/3 to 1/3 to 1/3 [1].

To evaluate the performance of the different elements making up this purifier, as well as its performance when using lower grade Ar as a source, we carried out the series of tests summarized below, liquifying purified Ar under different conditions:

a) using the complete system described above and Ar 60 as gas source, at low flow (15 l/min at STP);
b) same as a) but without the home-made molecular sieve filter;
c) same as b) but using liquid Ar 48 as a source (concentration of $O_2 \sim 1$ ppm, according to the supplier) instead of Ar 60;
d) a purifier built with large size cartridges[11] made for industrial applications and high flow (100 m^3/hour at STP): a dryer cartridge (HYDROSORB, containing a mixture of molecular sieves 4A and 13X) and a getter (OXISORB). The purifier was operated at high flow (120 l/min at STP) using commercial liquid Argon (Ar 48).

The results are plotted in Fig. 7. An electron lifetime larger than 4 milliseconds was achieved with all 4 four configurations listed above, corresponding to a purity level < 0.07 ppb O_2 equivalent.

In order to verify that these levels of purity do depend on the removal of electronegative impurities from the Ar gas while circulating through the purifier, Ar 60 was liquified *without purification*, i. e. directly from the gas bottle. The result is shown in Fig. 8. A stable value of lifetime

10 OXISORB Grosspatrone, Messer Griesheim GmbH, Dusseldorf, Germany.
11 HYDROSORB & OXISORB type R20, Messer Griesheim GmbH, Dusseldorf, Germany.

ranging from 60 to 120 μs was reached reproducibly within the same delay of about 10 hours, after recording an initial value of $\tau \approx 3$ μs; this latter value is roughly consistent with Argon 60 nominal concentration of O_2 (≤ 0.1 ppm). A similar effect has been reported in Ref. 7, where the spectra of a ^{207}Bi source in LAr was observed to take about 12 hours to stabilize after doping the LAr with N_2 and O_2.

5. The increase in electron lifetime after liquefaction

In an attempt to understand the increase in electron lifetime observed after liquefaction, several hypotheses were considered:

a) purification by means of photoemitted electrons that attach to electronegative impurities, causing them to drift towards the anode;
b) presence of microscopic powder (particles with linear dimensions of the order of several microns, coming from the filters that make up the purifier), that trap the electrons and slowly deposit at the bottom of the vessel;
c) Adsorption of contaminants on the surface of the chamber, taking place in a time scale governed by brownian motion.

The first of these hypotheses was discarded, because the ratio between the number of O_2 molecules present in the liquid and the number of photoelectrons generated per pulse is of the order of 10^{10}, and the repetition rate is orders of magnitude too small (typically ~ 1 min^{-1}) to achieve removal of the electronegative contaminants within the observed period.

In order to test the second and third hypothesis, we doped LAr with certain amounts of

1) O_2[12] with an impurity content, according to the supplier, of 200 ppm of N_2-Ar and 50 ppm of H_2O;
2) CO_2[13] with an impurity content of 16 ppm of N_2, 2 ppm of O_2 and 2 ppm of H_2O, specified by the supplier.

Neither of the two dopants was purified. The amount of gas was determined by introducing the dopant into a calibrated volume and measuring its pressure. Having filled about one half of the detector with purified LAr, the dopant was introduced into the cell by opening the

12 Medical Oxygen, Carbagas, Berne, Switzerland.
13 CO_2 48, Carbagas, Berne, Switzerland.

calibrated volume to the filling line of the cell, and completing afterwards the filling of the cell by condensing purified Ar. The concentration of dopant in LAr was calculated assuming that all the solute went in solution. The cell was equipped with a stirrer (a magnetized iron rod hermetically covered with teflon); the stirrer could be driven by an external rotating magnet.

The results of doping LAr with 3 ppb of O_2 and stirring are shown in Fig. 9; the result of doping LAr with 50 ppb of CO_2 is shown in Fig. 10.

A further test was carried out, by opening the calibrated volume containing 40 ppb of O_2 to the filling line of the cell, after the cell had been filled with purified Ar. The results are shown in Fig. 11. The results of this last test are in contradiction with hypothesis (b) mentioned above, for the O_2 contaminant was introduced in the cell *after* the cell had been filled (when τ was already a few milliseconds), *without* circulating the dopant through any of the filters comprising the purifier.

On the contrary, the results reported in Figs. 8-11 seem consistent with hypothesis (c).

5.1 Adsorption of impurities

The diffusion of impurities in LAr is a process governed by brownian motion. The average distance σ that a particle travels while performing a random walk is $\sigma = \sqrt{6Dt}$, where D is the diffusion coefficient and t is the time elapsed since the beginning of the random walk. The diffusion coefficient of (neutral) molecules in LAr should be similar to the diffusion coefficient of ions in the liquid. Since for an ion carrying a charge q, the diffusion coefficient D and the ion mobility μ obey the Einstein relation, $D = \mu(kT/q)$, the knowledge of the ion mobility at LAr temperatures, $\mu \sim 5 \cdot 10^{-2}$ $cm^2V^{-1}s^{-1}$, permits an estimation of D for neutral molecules, $D \sim 7 \cdot 10^{-5}$ cm^2s^{-1}. This estimation suggests that molecules diffusing in LAr could travel a distance comparable to the radius of the cell (~ 3 cm) in a few hours.

The decrease in electron lifetime τ (taking place in about 10 hours) displayed in Fig. 11, is consistent with this estimation and suggests that, indeed, the diffusion of impurities over distances of the order of the linear dimensions of the cell takes place in a time scale of a few hours. The increase in τ displayed in Figs. 8-10 can then be interpreted as adsorption of electron-attaching molecules on the walls of the cell; the time it takes for the impurities to diffuse across the cell is the time necessary to reach a stable reading of τ. The positive jumps in electron lifetime observed

when stirring (Fig. 9) would correspond to an increase of the probability of impurity molecules colliding with the walls, provided that the sticking probability of an O_2 molecule to stainless steel is larger than that of an Ar atom. The change in τ observed in LAr doped with 3 ppb of O_2 (Fig. 9) corresponds to adsorption of < 1/10 of a monolayer of O_2.

6. Electric field dependence of the electron lifetime in LAr

Using the monitoring system described above, we measured the electric field dependence of the electron lifetime in LAr doped with O_2 and CO_2; the results are displayed in Fig. 12.

From this data, the rate constant for the reaction $e^- + X \xrightarrow{k_X} X^-$ can be calculated as $k_X = \{\tau [X]\}^{-1}$, where [X] is the molar concentration of solute X and t is the electron lifetime observed in LAr when doped with [X] moles of solute X. In the case $X = O_2$, at a field E = 800 V/cm, the rate constant k_{O_2} calculated from our data, agrees within 10 % with the value reported in Ref. 8, indicating that our estimation of the concentration of dopant dissolved in LAr is not too bad. Furthermore, k_{O_2} *decreases* with increasing electric field, a trend which is consistent with that displayed in Fig. 2 of Ref. 8.

In the case $X = CO_2$ at E = 100 V/cm, the rate constant k_{CO_2} calculated from our data (assuming that electrons attach to CO_2 dissolved in LAr) corresponds to $k_{CO_2} = 5.3 \cdot 10^9$ M^{-1} s^{-1}, almost two orders of magnitude smaller than k_{O_2} at the same field strength. Furthermore, contrary to the case of k_{O_2}, k_{CO_2} *increases* with increasing field strength, reaching a value of $k_{CO_2} = 1.6 \cdot 10^{10}$ $M^{-1}s^{-1}$ at a field of 800 V/cm.

7. Conclusions

A small drift monitoring chamber suited for measurements of the electron lifetime τ in LAr has been successfully tested. Several tests performed with different purification systems lead to the conclusion that commercially available filters (e. g. a dryer and an OXISORB getter cartridge) operating at high flow are adequate for purifying Ar to a level of < 0.1 ppb of O_2 equivalent (τ > 4 ms).

The increase in electron lifetime observed after liquefaction of purified Ar is consistent with adsorption of electronegative impurities on the surface of the detector, a process governed by thermal diffusion.

Acknowledgements

We gratefully acknowledge the support of the Istituto Nazionale di Fisica Nucleare for having funded this work. Thanks are also due to CERN for the hospitality in its stimulating environment and to the people who have helped in the preparation of the work described here: M. Benvenuto, A. Galvani, S. Lasic, R. Pavanello, H. Rigoni and M. Santoni.

The authors are grateful to K. Geissler for fruitful discussions and technical support.

Table 1. *Voltages, fields and transit times corresponding to a drifting field between cathode grid and anode grid of 400 V/cm.*

V_{cath} = -1080 V	E_{cath} = 160 V/cm	T_{cath} = 7 μs
$V_{grid\ cath}$ = -1000 V $V_{grid\ anod}$ = +1000 V	E_{drift} = 400 V/cm	T_{drift} = 34 μs
V_{anod} = +1500 V	E_{anod} = 1000 V/cm	T_{anod} = 3 μs

Table 2. *Voltages, fields and transit times corresponding to a drifting field between cathode grid and anode grid of 50 V/cm.*

V_{cath} = -135 V	E_{cath} = 20 V/cm	T_{cath} = 42 μs
$V_{grid\ cath}$ = -125 V $V_{grid\ anod}$ = +125 V	E_{drift} = 50 V/cm	T_{drift} = 183 μs
V_{anod} = +187 V	E_{anod} = 125 V/cm	T_{anod} = 20 μs

References

[1] E. Buckley et al., Nucl. Instr. and Meth. **A275** (1989) 364.
[2] S. Bonetti et al., Nucl. Instr. and Meth. **A286** (1990) 135.
[3] G. Carugno et al., Nucl. Instr. and Meth. **A292** (1990) 580
[4] R. Reininger et al., Phys. Rev. **B28** (1983) 4426.
[5] A.G. Mathewson, CERN-ISR-VA 74-10, 74-30, CERN-LEP-VA 87-63 and M.H. Achard et al., Vacuum **29**(2) (1978) 53.
[6] Y. E. Strausser, "Review of outgassing results", VARIAN Vacuum Division, VR 51 (1968) and "Proceedings of the 4th Int. Vacuum Congress", Manchester, U.K. (1968).
[7] S. D. Biller et al., Nucl. Instr. and Meth. **A276** (1989) 144.
[8] G. Bakale, U. Sowada and W. F. Schmidt, J. Phys. Chem. **80** (1976) 2556.

Figure captions

Fig. 1. Cross-section of the monitoring chamber. The dimensions are in mm.

Fig. 2. Layout of the system, including a schematic representation of the connections of the chamber to the laser and to the front-end electronics, signal processing and data acquisition.

Fig. 3. The electric field lines and the equipotential contour in the half cross section of the chamber as a result of a computer simulation. The trajectories of the electrons extracted from the photocathode are also shown as bold lines parallel to the electric field. Notice that the photocathode extends in a region where only rectilinear trajectories are generated.

Fig. 4. Two typical output signals as they appear on a Macintosh screen. All the parameters used on the off-line analysis program are also indicated: Q_C and Q_A are the integrated charge at the cathode and anode, respectively; T_C is the time required by the electrons to drift from the cathode to its facing grid; T_A the time to drift from the grid facing the anode to the anode itself; T_D the drift time between the two grids; T_w the FWHM of the overall signal.

Fig. 5. The error on the lifetime versus the ratio between the integrated charge at the anode and at the cathode, Q_A/Q_C, assuming a constant error $\Delta T_w/T_w \sim 5\%$ (the minimum in the curve is mainly due to this error). A 10% uncertainty on τ corresponds to a charge ratio $0.08 < R < 0.76$.

Fig. 6. The ratio between the integrated charge at the anode and at the cathode, as a function of the electron lifetime, for E=400V/cm and E=50 V/cm. The 10% error boundaries on the lifetime (15 $\mu s < \tau < 900$ μs) on a single measurement are graphically determined assuming that the charge ratio R is in the range indicated in Fig. 5.

Fig. 7. Lifetime measurements performed with 3 different purifier configurations as a function of the elapsed time after liquefaction. The result ($\tau > 4$ ms), obtained for all of them, corresponds to a purity level ≤ 0.1 ppb of oxygen equivalent.

Fig. 8. Measurement of electron lifetime τ in Ar 60 *without* any purification. A delay of about 10 hours can be seen between the end of the liquefaction process, and the time after which a stable value of lifetime ($\tau \approx 70$ μsec) is achieved. Notice that the initial value of $\tau \sim 3$ μs, measured during or at the end of the liquefaction process, is roughly consistent with the O_2 content of Ar 60 specified by the supplier.

Fig. 9. Electron lifetime τ measured in LAr doped with 3 ppb of O_2. The O_2 was introduced into the cell after it had been half filled with purified Ar. The jumps in τ are due to stirring (lasting between 20 to 60 min). The measurement was stopped when there was no more change in τ after stirring.

Fig. 10. Electron lifetime τ measured in LAr doped with 50 ppb of CO_2. The CO_2 was introduced into the cell after it had been half filled with purified LAr.

Fig. 11. Electron lifetime τ measured in LAr doped with 40 ppb of O_2. The O_2 was introduced into the cell (in the gas phase) 250 min after it had been filled with purified LAr.

Fig. 12. Electric field dependence of the electron lifetime τ in purified LAr doped with 40 ppb CO_2 and 3.5 ppb O_2. Lines are drawn to guide the eye.

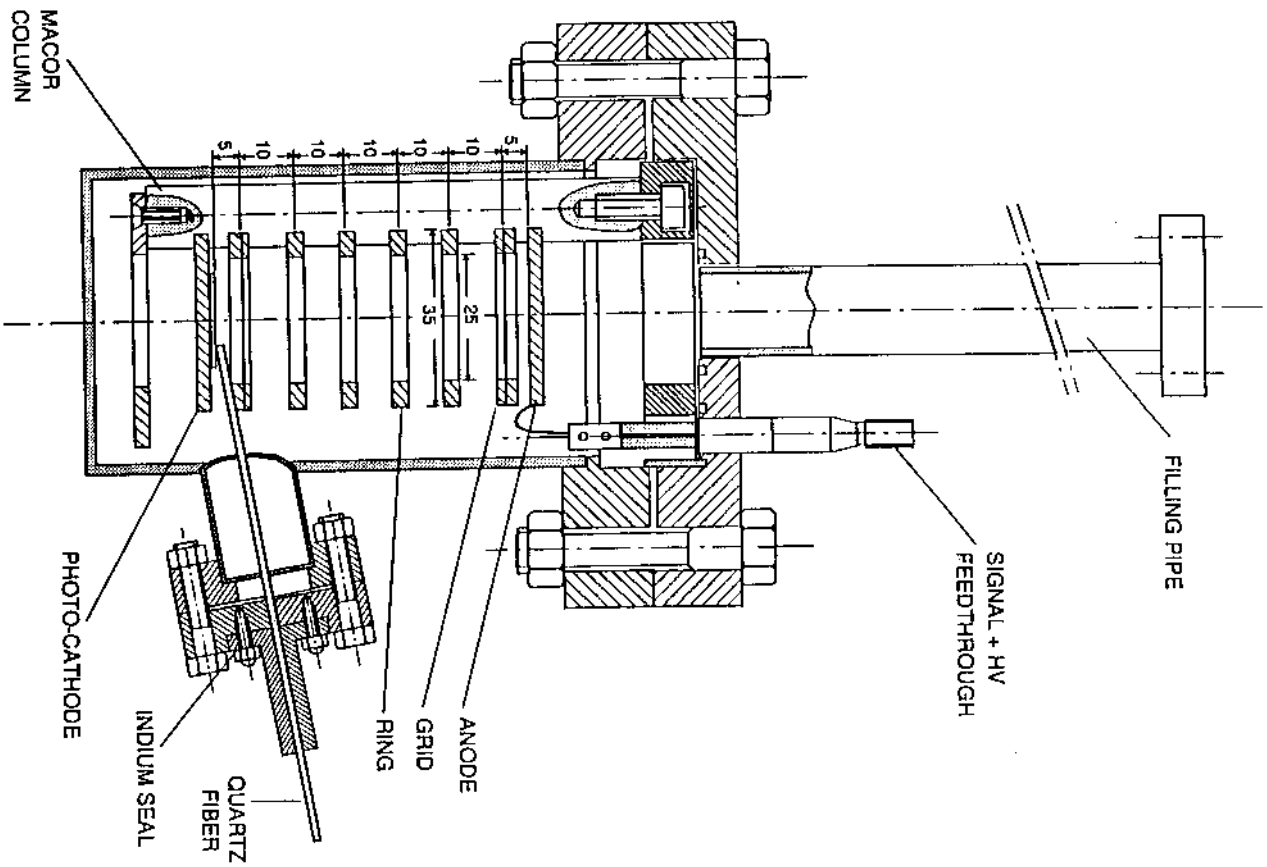
MACOR COLUMN
5
10
10
10
10
10
5
35
25
PHOTO-CATHODE
INDIUM SEAL
QUARTZ FIBER
RING
GRID
ANODE
SIGNAL + HV FEEDTHROUGH
FILLING PIPE

Fig. 1

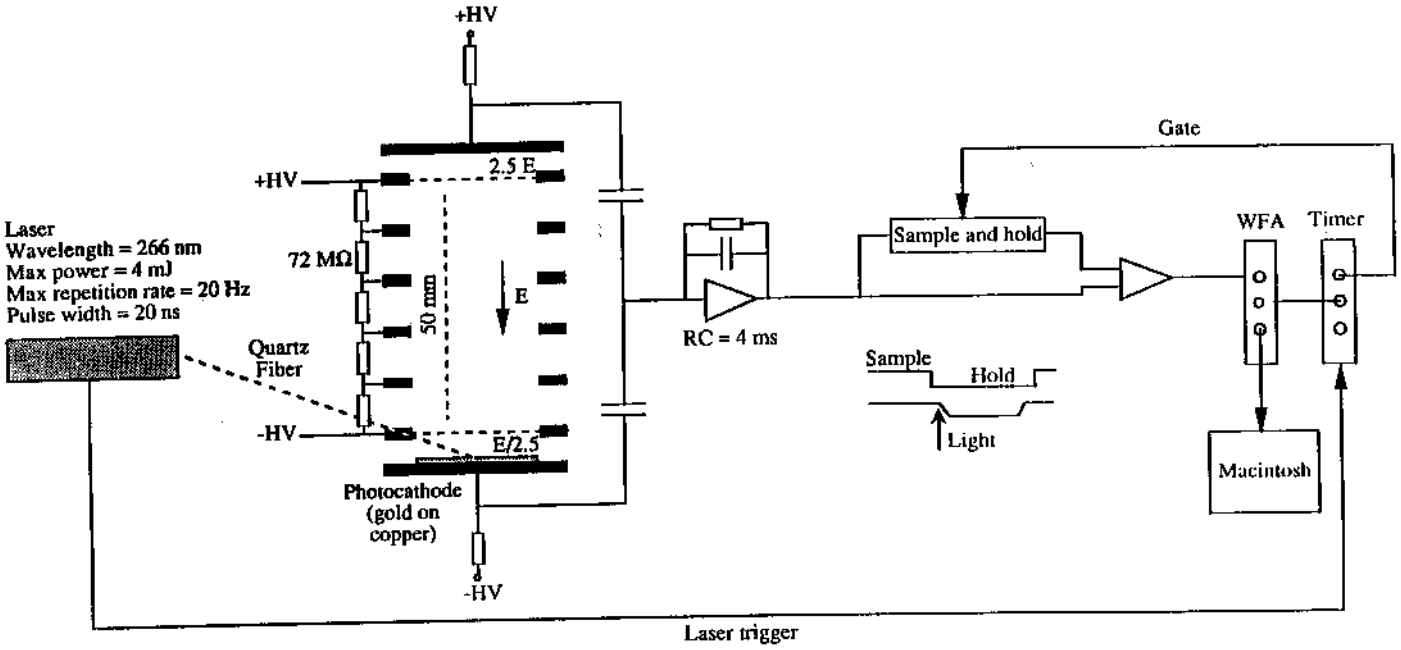
+HV
2.5 E
+HV
72 MΩ
50 mm
E
Laser
Wavelength = 266 nm
Max power = 4 mJ
Max repetition rate = 20 Hz
Pulse width = 20 ns
Quartz Fiber
-HV
E/2.5
Photocathode (gold on copper)
-HV
RC = 4 ms
Gate
Sample and hold
WFA
Timer
Sample
Hold
Light
Macintosh
Laser trigger

Fig. 2

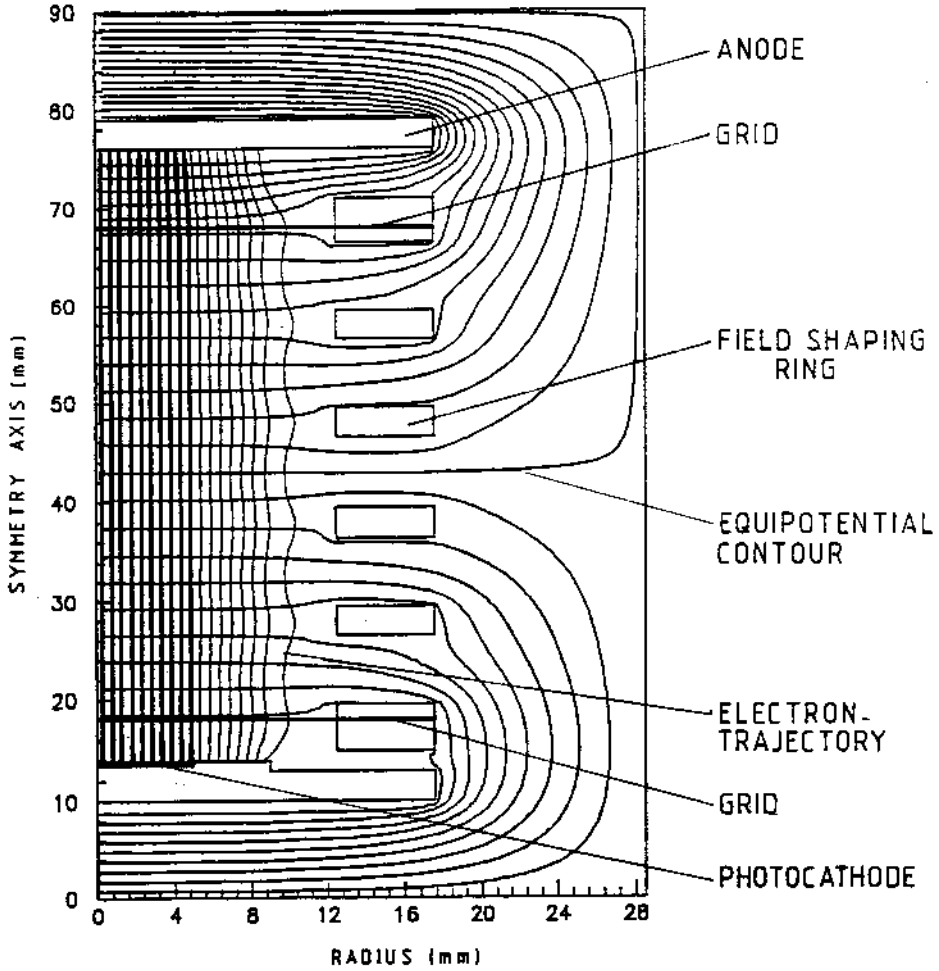
ANODE
GRID
FIELD SHAPING RING
EQUIPOTENTIAL CONTOUR
ELECTRON-TRAJECTORY
GRID
PHOTOCATHODE
SYMMETRY AXIS (mm)
RADIUS (mm)
0
10
20
30
40
50
60
70
80
90
0
4
8
12
16
20
24
28

Fig. 3

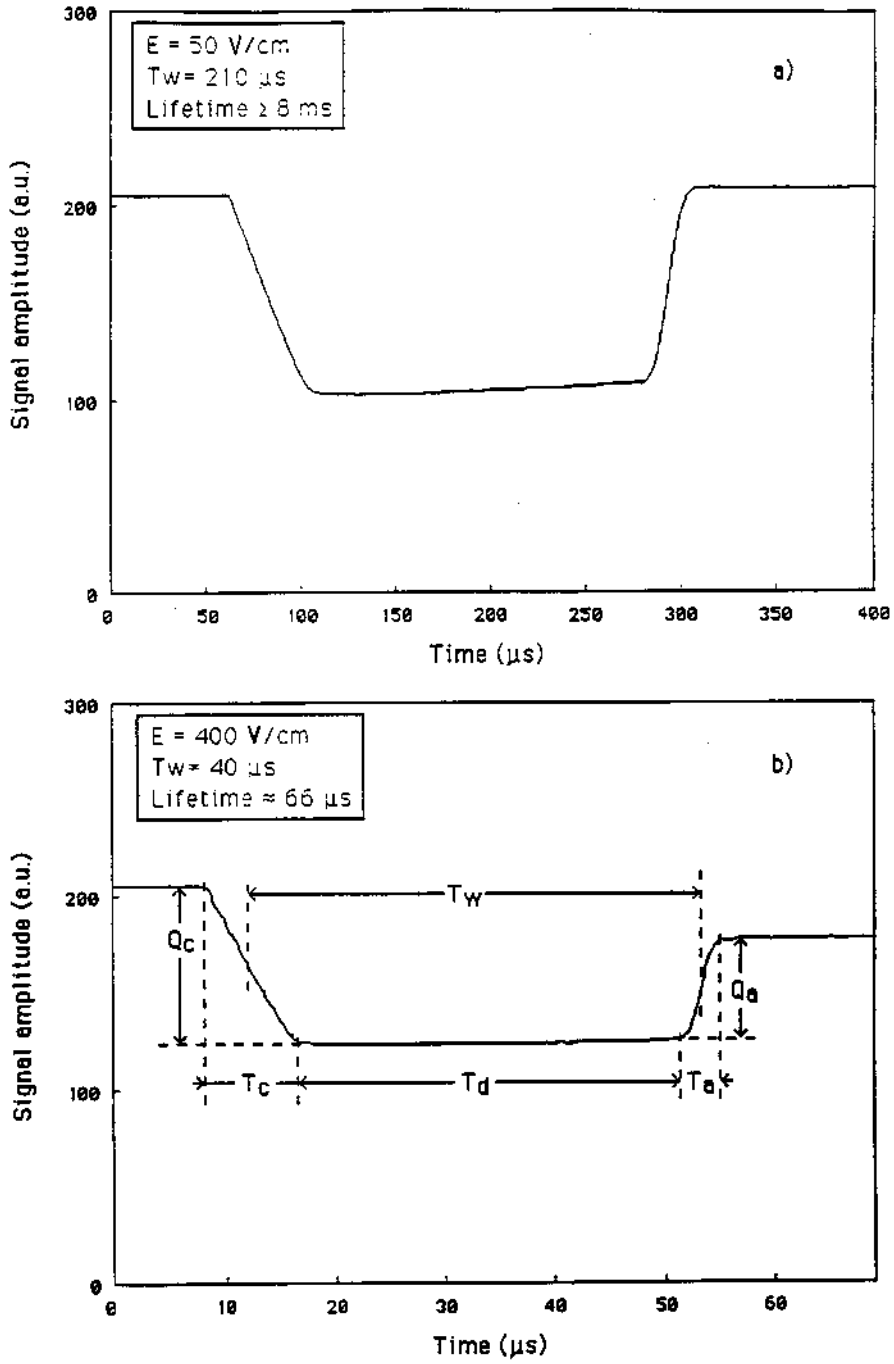
E = 50 V/cm
Tw= 210 µs
Lifetime ≥ 8 ms
a)
Signal amplitude (a.u.)
Time (µs)
E = 400 V/cm
Tw= 40 µs
Lifetime ≈ 66 µs
b)
Qc
Tw
Qa
Tc
Td
Ta
Signal amplitude (a.u.)
Time (µs)

Fig. 4

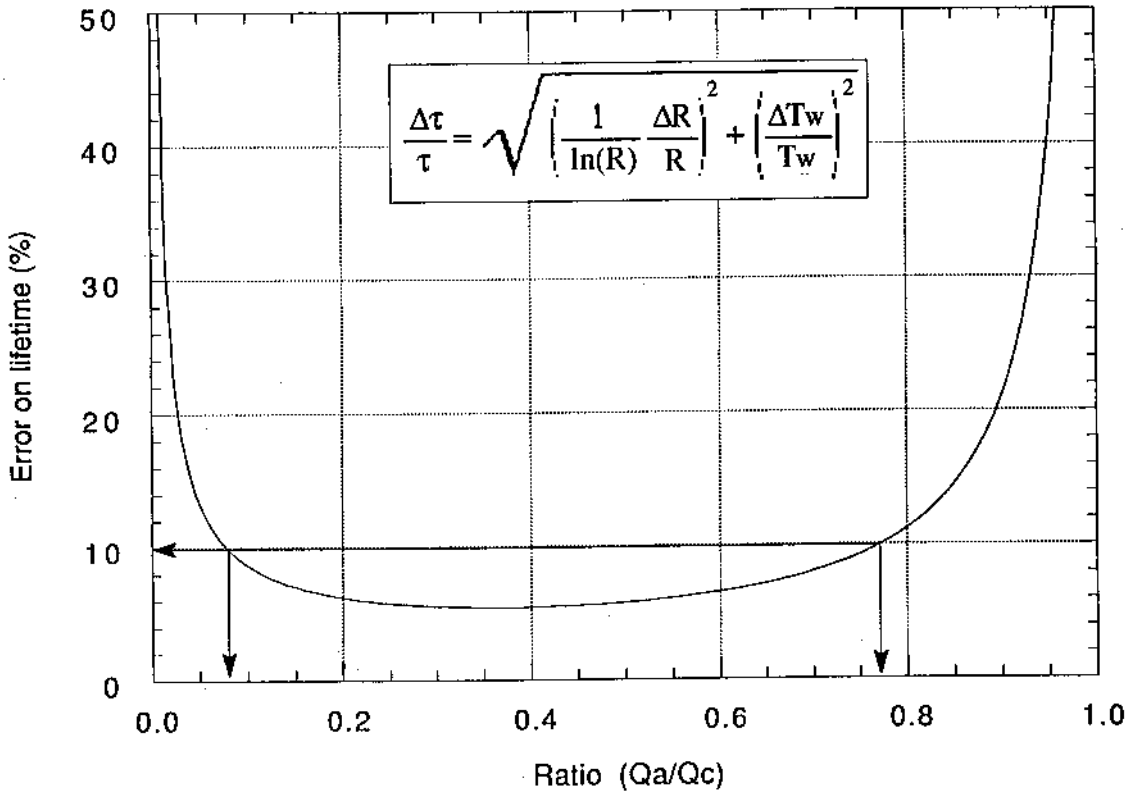
$\frac{\Delta\tau}{\tau} = \sqrt{\left|\frac{1}{\ln(R)}\frac{\Delta R}{R}\right|^2 + \left|\frac{\Delta Tw}{Tw}\right|^2}$
Error on lifetime (%)
50
40
30
20
10
0
0.0
0.2
0.4
0.6
0.8
1.0
Ratio (Qa/Qc)

Fig. 5

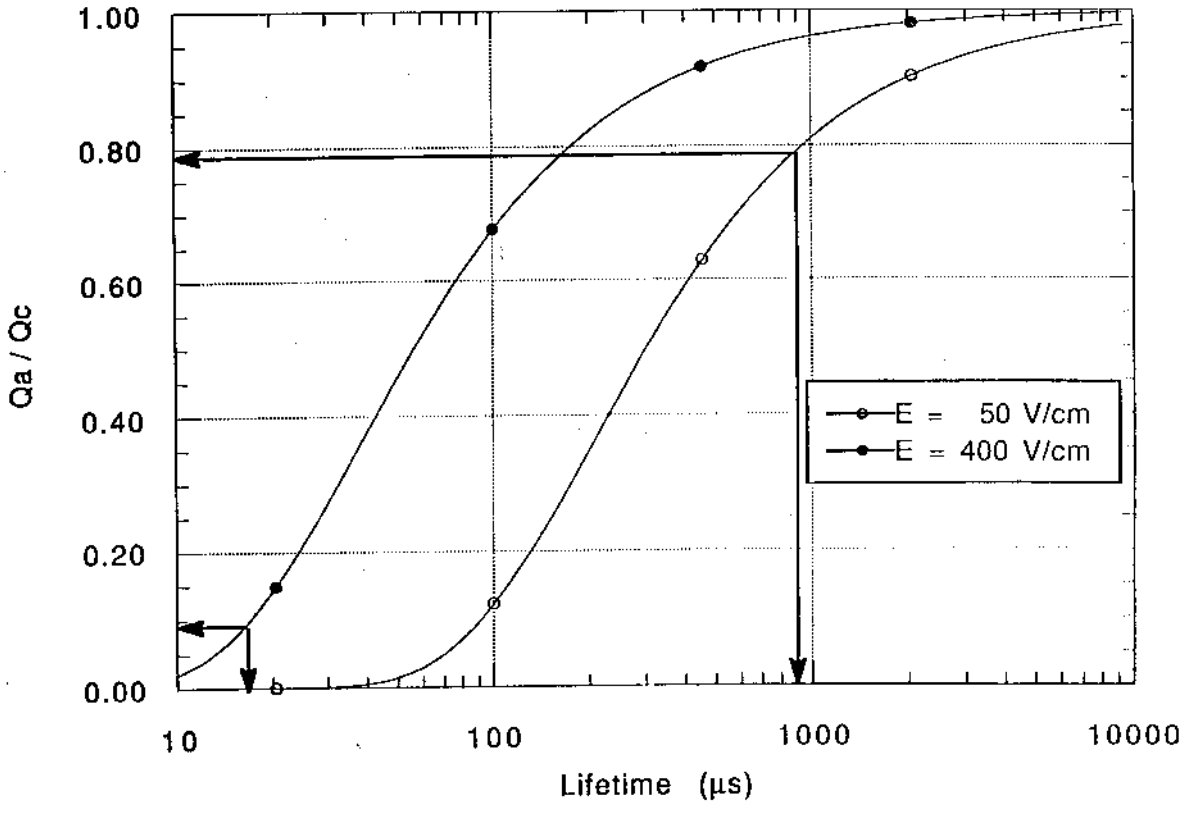
Qa / Qc
1.00
0.80
0.60
0.40
0.20
0.00
10
100
1000
10000
Lifetime (µs)
E = 50 V/cm
E = 400 V/cm

Fig. 6

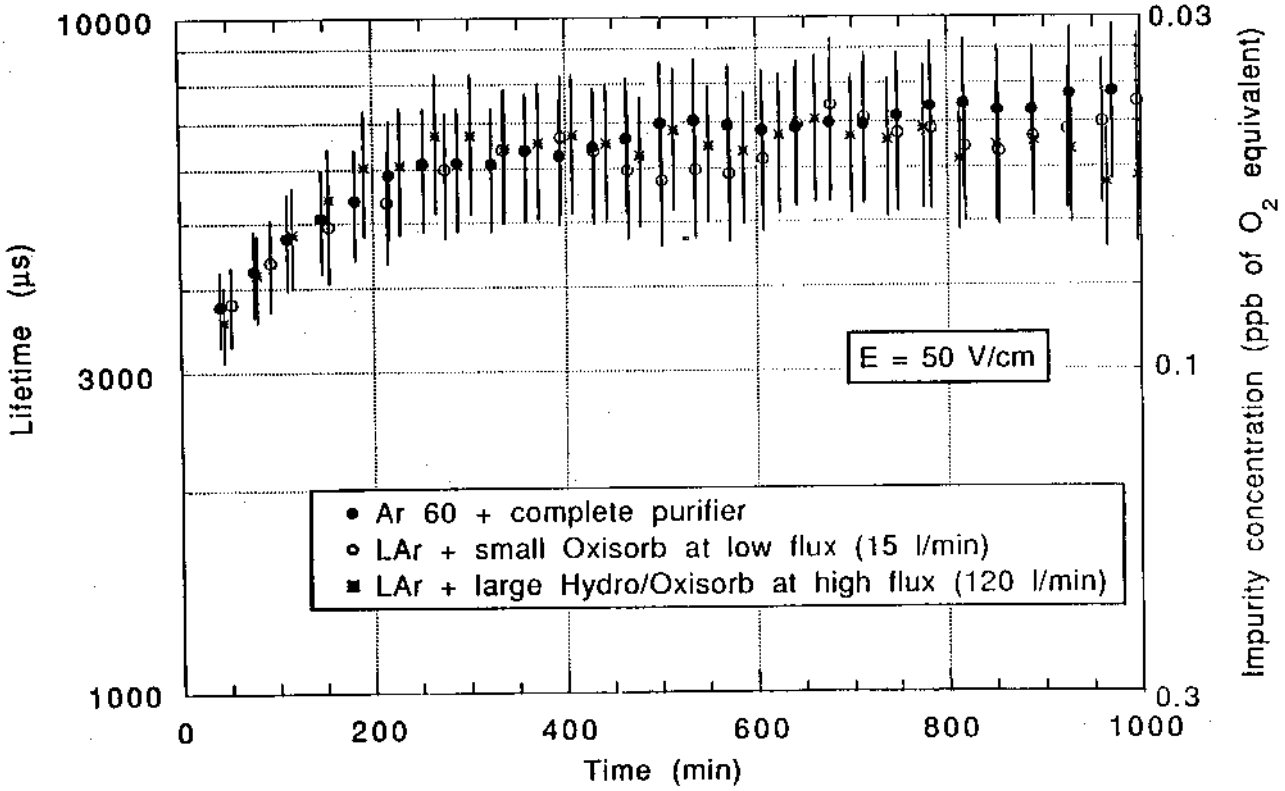
10000
3000
1000
Lifetime (μs)
0.03
0.1
0.3
Impurity concentration (ppb of O_2 equivalent)
E = 50 V/cm
• Ar 60 + complete purifier
○ LAr + small Oxisorb at low flux (15 l/min)
■ LAr + large Hydro/Oxisorb at high flux (120 l/min)
0
200
400
600
800
1000
Time (min)

Fig. 7

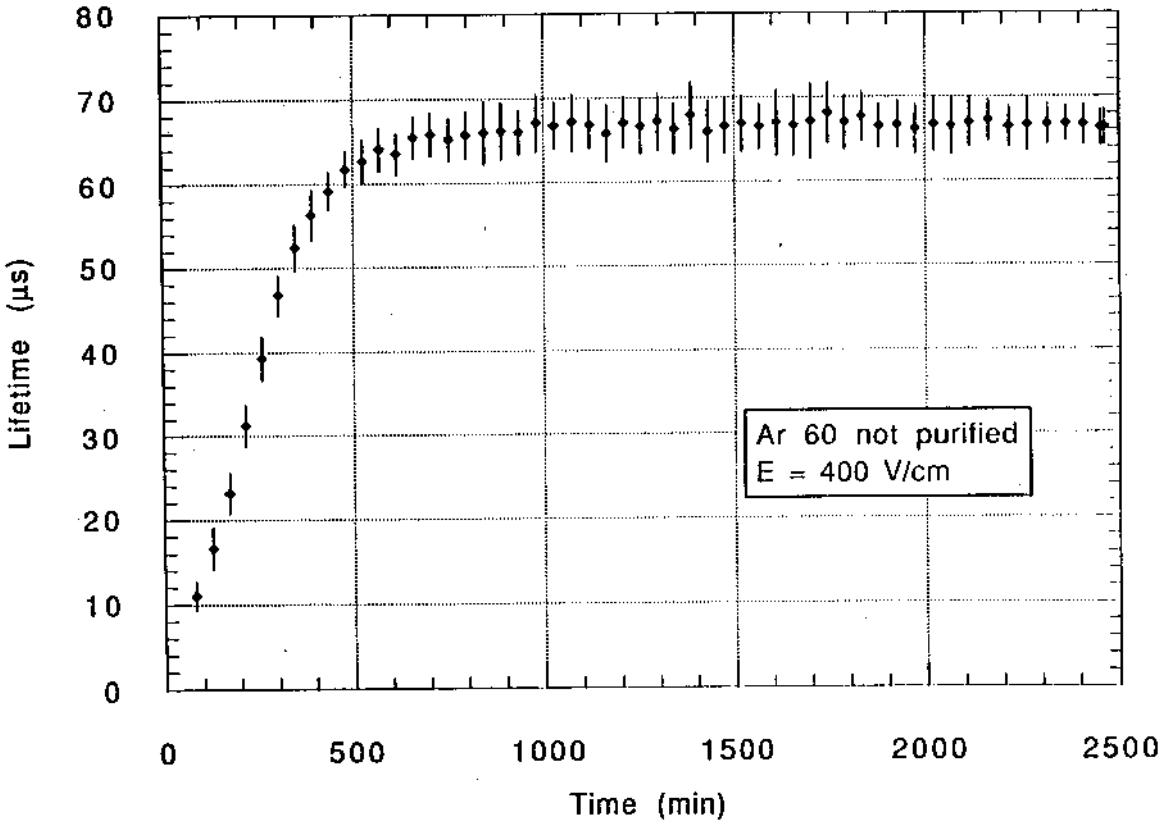
80
70
60
50
40
30
20
10
0
Lifetime (μs)
Ar 60 not purified
E = 400 V/cm
0
500
1000
1500
2000
2500
Time (min)

Fig. 8

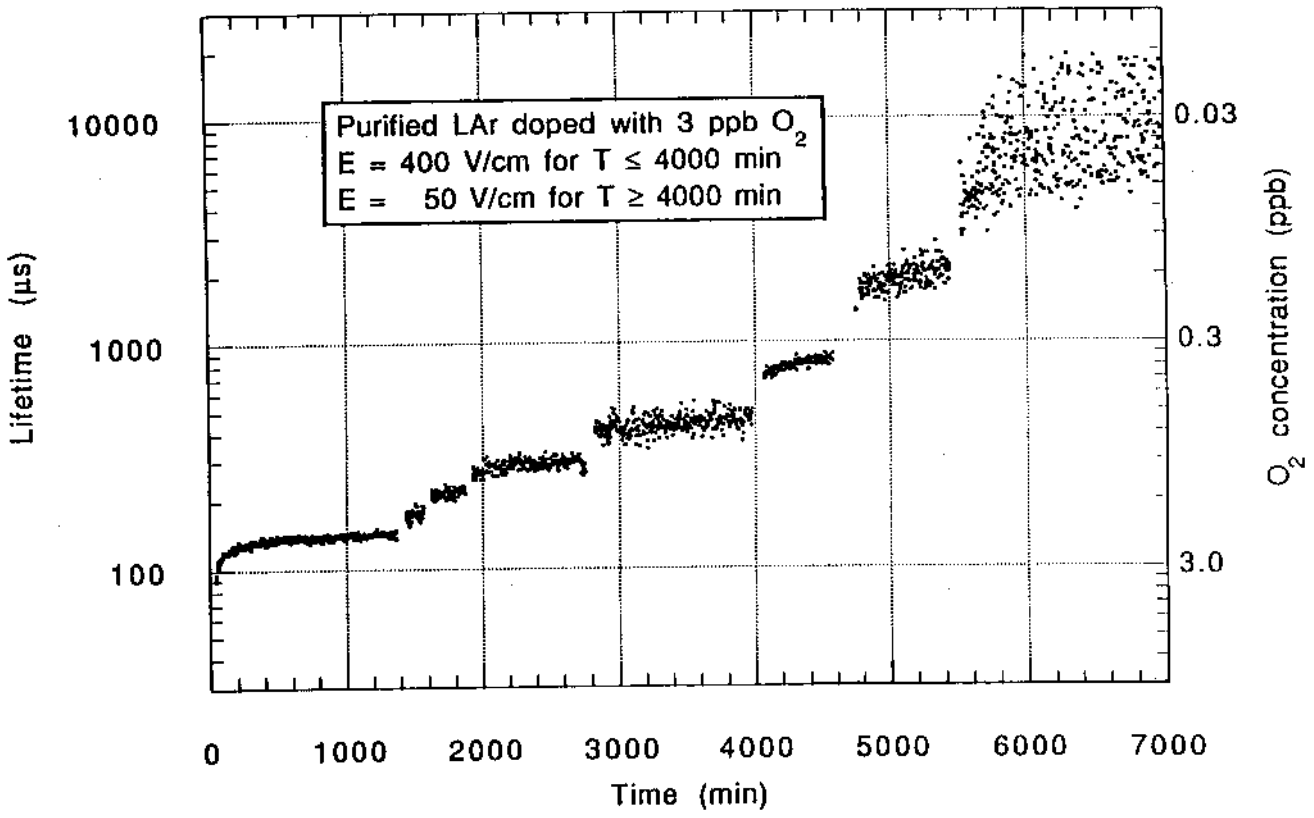
Purified LAr doped with 3 ppb O_2
E = 400 V/cm for T ≤ 4000 min
E = 50 V/cm for T ≥ 4000 min
Lifetime (μs)
10000
1000
100
0.03
0.3
3.0
O_2 concentration (ppb)
0
1000
2000
3000
4000
5000
6000
7000
Time (min)

Fig. 9

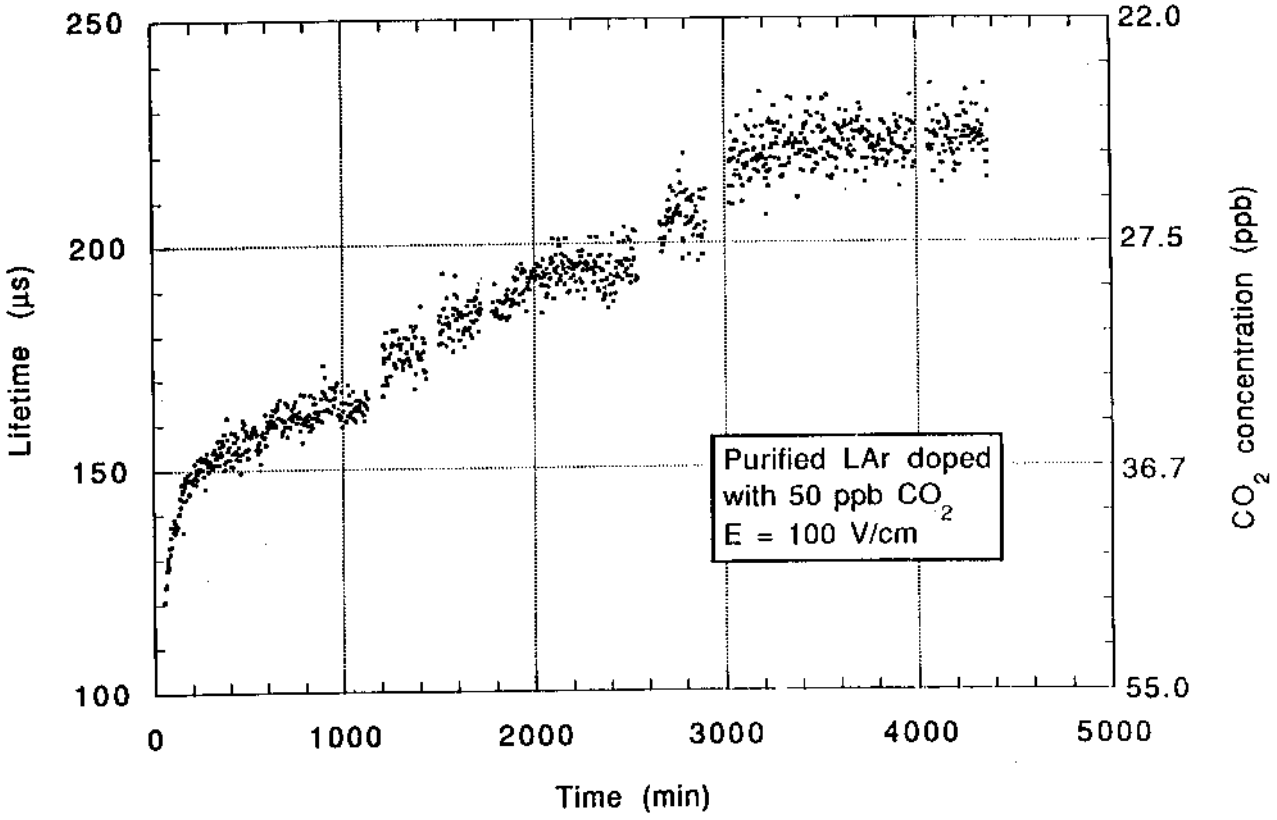
Purified LAr doped
with 50 ppb CO_2
E = 100 V/cm
Lifetime (μs)
250
200
150
100
22.0
27.5
36.7
55.0
CO_2 concentration (ppb)
0
1000
2000
3000
4000
5000
Time (min)

Fig. 10

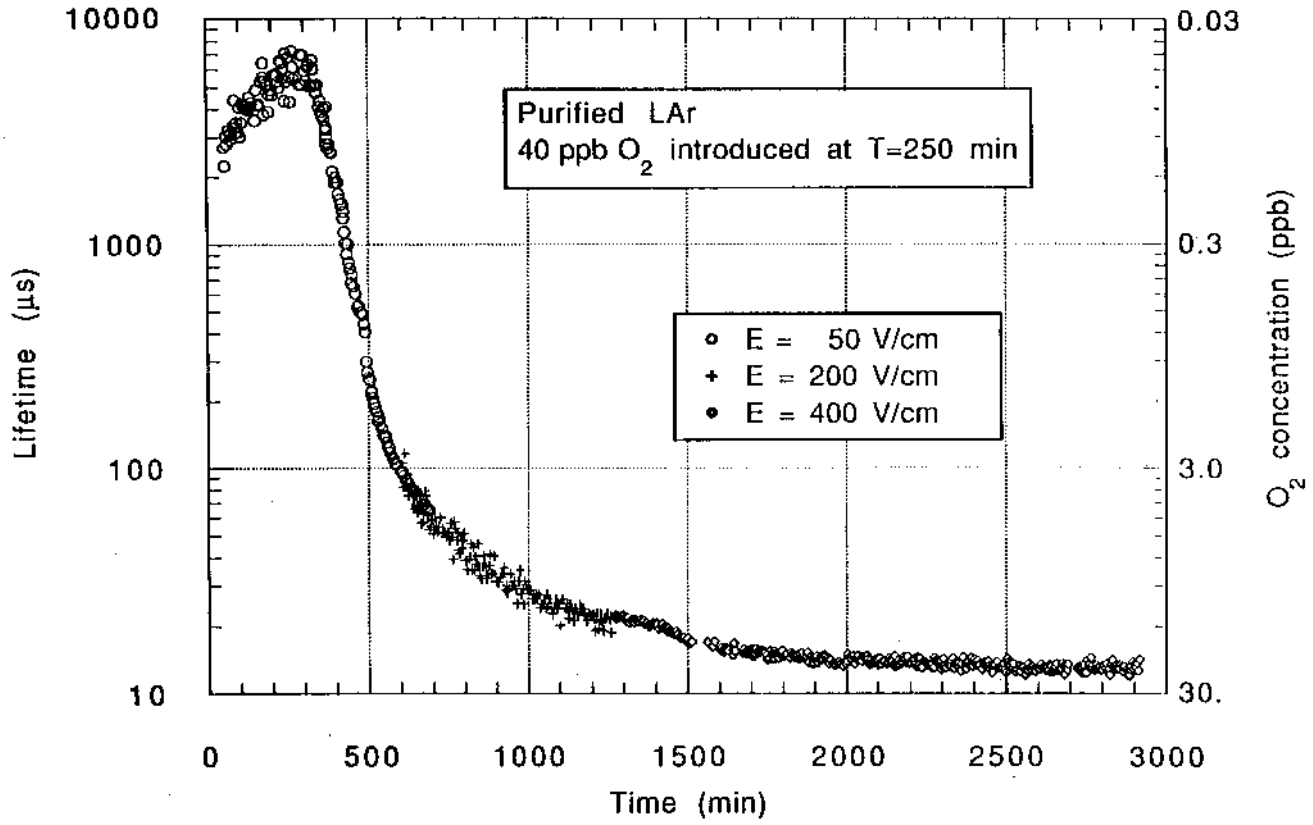
Purified LAr
40 ppb O_2 introduced at T=250 min
E = 50 V/cm
E = 200 V/cm
E = 400 V/cm
Lifetime (µs)
O_2 concentration (ppb)
Time (min)
10000
1000
100
10
0.03
0.3
3.0
30.
0
500
1000
1500
2000
2500
3000

Fig. 11

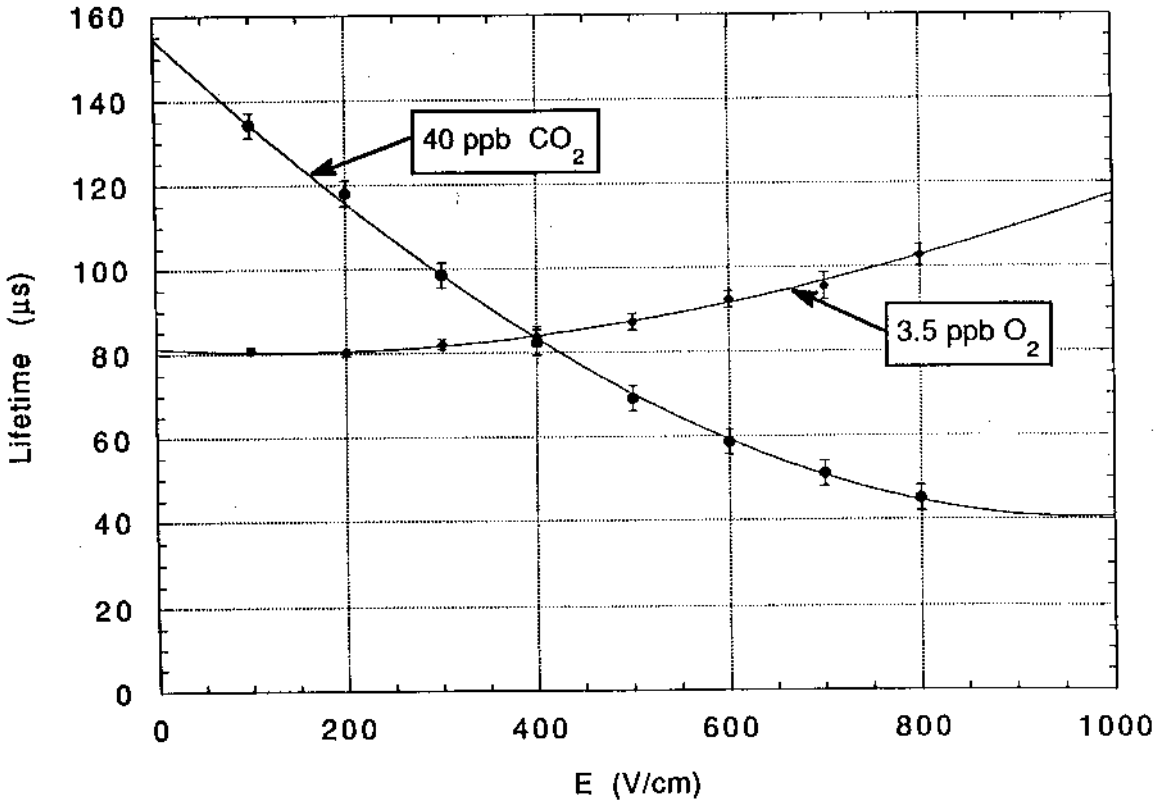
40 ppb CO_2
3.5 ppb O_2
Lifetime (µs)
E (V/cm)
160
140
120
100
80
60
40
20
0
0
200
400
600
800
1000

Fig. 12